

Single crystal growth and magnetic anisotropy characterization of Ising-like antiferromagnets Na_4MTeO_6 (M = Co, Ni)

Yuerui Chen(陈月瑞), Suiman Fu(付随满), Zhiying Zhao(赵志颖), Meiyan Cui(崔美艳), and Zhangzhen He(何长振)

Citation: Chin. Phys. B, 2026, 35 (**8**): 086803. DOI: 10.1088/1674-1056/ae40dd
http://cpb.iphy.ac.cn; http://iopscience.iop.org/cpb

What follows is a list of articles you may be interested in

Magnetic anisotropy in MnGe thin films and its evolution under external magnetic fields

Zhaohang Li(李朝航), Fanbao Meng(孟凡保), Kesen Zhao(赵科森), Tao Qi(齐涛), Shihao Liu(刘仕豪), Zongyao Huang(黄宗耀), Feixiong Quan(全飞熊), Zhiwei Wang(王智炜), Zhengjie Wang(王郑杰), Xigang Luo(罗习刚), Jianjun Ying(应剑俊), Yubin Hou(侯玉斌), Wenjie Meng(孟文杰), Qingyou Lu(陆轻铀), and Xianhui Chen(陈仙辉)

Chin. Phys. B, 2026, 35 (**1**): 016802. DOI: 10.1088/1674-1056/ae1191

Modeling of microstructure and microsegregation evolution in solidification of ternary alloys

Qiannan Yu(于芊楠), Mengdan Hu(胡梦丹), Jinyi Wu(吴津仪), and Dongke Sun(孙东科)

Chin. Phys. B, 2025, 34 (**5**): 056801. DOI: 10.1088/1674-1056/adb8b5

Influences of divalent ion substitution on the magnetic and dielectric properties of W-type barium ferrite

Shiyue He(何诗悦), Ruoshui Liu(刘若水), Xujie Liu(刘煦婕), Xianping Ye(叶先平), Lichen Wang(王利晨), and Baogen Shen(沈保根)

Chin. Phys. B, 2024, 33 (**6**): 066801. DOI: 10.1088/1674-1056/ad39d5

High repetition granular Co/Pt multilayers with improved perpendicular remanent magnetization for high-density magnetic recording

Zhi Li(李智), Kun Zhang(张昆), Ao Du(杜奥), Hongchao Zhang(张洪超), Weibin Chen(陈伟斌), Ning Xu(徐宁), Runrun Hao(郝润润), Shishen Yan(颜世申), Weisheng Zhao(赵巍胜), and Qunwen Leng(冷群文)

Chin. Phys. B, 2023, 32 (**2**): 026803. DOI: 10.1088/1674-1056/ac9fc1

Effects of dielectric decrement on surface potential in a mixed electrolyte solution

Jing Peng(彭景), Wen-Xin Zou(邹温馨), Rui Tian(田锐), Hang Li(李航), Xin-Min Liu(刘新敏)

Chin. Phys. B, 2018, 27 (**12**): 126801. DOI: 10.1088/1674-1056/27/12/126801

Single crystal growth and magnetic anisotropy characterization of Ising-like antiferromagnets Na_4MTeO_6 (M = Co, Ni)

Yuerui Chen(陈月瑞)[1,2], Suiman Fu(付随满)[1,3], Zhiying Zhao(赵志颖)[1], Meiyan Cui(崔美艳)[1], and Zhangzhen He(何长振)[1,†]

[1] *State Key Laboratory of Functional Crystals and Devices, Fujian Institute of Research on the Structure of Matter, Chinese Academy of Sciences, Fuzhou* 350002, *China*

[2] *College of Physics and Energy, Fujian Normal University, Fuzhou* 350117, *China*

[3] *College of Chemistry and Materials Science, Fujian Normal University, Fuzhou* 350117, *China*

(Received 9 December 2025; revised manuscript received 27 January 2026; accepted manuscript online 3 February 2026)

Large-sized single crystals of Na_4MTeO_6 (M = Co, Ni) were successfully grown using the flux method. The magnetic anisotropy and field-induced magnetic transitions were systematically investigated, and the distortion of the CoO_6 and NiO_6 octahedra was quantitatively analyzed. Both compounds are identified as strongly anisotropic Ising-like antiferromagnets. Na_4CoTeO_6 exhibits a Néel temperature of 3.2 K with the b-axis as the easy axis, and field-induced spin-flip transitions are observed along all three crystallographic directions. The magnetic anisotropy constant is determined to be $K(2\ \mathrm{K}) = 1.63(5) \times 10^5$ erg/cm^3. In Na_4NiTeO_6, the Néel temperature is 5.9 K, also with the b-axis as the easy axis, while field-induced spin-flip transitions occur along both the a- and b-axes, yielding an anisotropy constant of $K(2\ \mathrm{K}) = 1.63(4) \times 10^4$ erg/cm^3. Structural analysis reveals that the Co^{2+} ions in Na_4CoTeO_6 exhibit larger bond-length and bond-angle distortions within the CoO_6 octahedra than the Ni^{2+} ions in Na_4NiTeO_6. These results highlight the significant role of octahedral distortion in governing the strong magnetic anisotropy of the Na_4MTeO_6 family.

Keywords: Ising-like antiferromagnets, single crystal growth, magnetic anisotropy

PACS: 68.08.De, 75.50.–y, 75.50.Ee

DOI: 10.1088/1674-1056/ae40dd **CSTR:** 32038.14.CPB.ae40dd

1. Introduction

Ising-like systems serve as a bridge connecting the Ising and Heisenberg models.[1,2] Ising-like antiferromagnets, characterized by their strong magnetic anisotropy and unique spin configurations, exhibit a series of unconventional physical phenomena that challenge traditional understanding. These phenomena not only deepen our knowledge of low-dimensional magnetic order[3,4] and quantum effects,[5] but also provide theoretical foundations for the development of spintronic devices. The $S = 1/2$ Ising-like chain is commonly found in cobalt oxides due to the Kramers nature of Co^{2+} ions,[6,7] leading to a variety of intriguing quantum phenomena such as quantum criticality[8–10] and Bethe strings.[11] For example, as an Ising-like system, $SrCo_2V_2O_8$[12,13] exhibits an intermediate state dominated by quantum fluctuations at low temperatures, with its excitation spectrum characterized by the coexistence of Ising-type energy gaps and XY-type continuous excitations. Consequently, it serves as an ideal platform for investigating the evolution of one-dimensional quantum magnetic anisotropy. In $CoNb_2O_6$, quantum critical magnetic excitations[14–16] and E_8 symmetry excitations[17,18] have been observed. By contrast, $NiNb_2O_6$ shows similar quantum critical excitations[19] but is not an Ising–like-type antiferromagnet.

Compared with Co^{2+} ($3d^7$) ions, which possess a single electron in the e_g orbital, Ni^{2+} ($3d^8$) ions have two electrons occupying the e_g orbitals, resulting in a more stable octahedral crystal-field configuration. Therefore, the NiO_6 octahedra are not prone to deformation, making it difficult to form strong magnetic anisotropy, and thus Ising-like system antiferromagnetism, extremely rare in Ni-based oxides. This rarity renders Ni-based Ising-like systems highly valuable for exploration. For instance, in $Na_2Ni_2TeO_6$,[20] Ni^{2+} forms quasi-1D chains (intrachain XY coupling; interchain weak Ising antiferromagnetic coupling). Neutron scattering shows coexisting XY continuous excitations and Ising gaps, partial bistability with relaxation, a model for 1D anisotropy competition. Therefore, investigating Ising-like antiferromagnets in cobalt and nickel oxides offers a promising pathway to uncover exotic magnetic behaviors and to provide real-material platforms for studying theoretical models.

In our previous work,[21,22] we have successfully synthesized the family of Na_4MTeO_6 (M = Co, Ni) single crystals. As the first example of one-dimensional (1D) chain-like tellurates, Na_4CoTeO_6 and Na_4NiTeO_6 crystallize in the monoclinic $P2/c$ and triclinic P-1 space groups, respectively, forming quasi-1D zigzag spin chains along the c- and a-axes. Magnetic susceptibility measurements on polycrys-

†Corresponding author. E-mail: hezz@fjirsm.ac.cn

© 2026 Chinese Physical Society and IOP Publishing Ltd. All rights, including for text and data mining, AI training, and similar technologies, are reserved.

talline samples confirmed that both compounds possess antiferromagnetic ground states and exhibit field-induced magnetic transitions.[21] However, due to the rough surface and flake-like morphology of Na_4CoTeO_6 crystals, as well as the presence of a small amount of black impurities inside Na_4NiTeO_6 crystals, it is difficult to select suitable crystals for the measurement of magnetic anisotropy. Subsequent neutron powder diffraction and first-principles calculations on Na_4NiTeO_6 revealed that Ni^{2+} ions form a helical ferromagnetic zigzag chain along the a-axis, which are antiferromagnetically coupled along the b- and c-axes.[23]

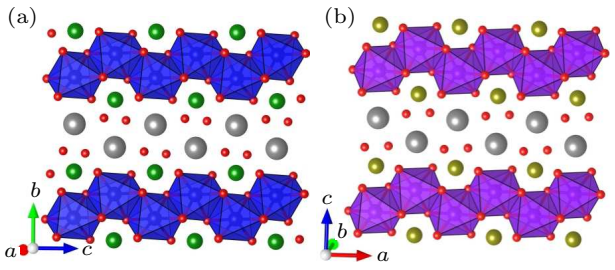


Fig. 1. Crystal structures of Na_4MTeO_6 (M = Co, Ni): (a) Na_4CoTeO_6 shows a uniform zigzag chain structure along the c-axis, built by blue polyhedra CoO_6, where gray, green, and red balls represent Na, Te, and O atoms, respectively. (b) Na_4NiTeO_6 exhibits an alternating zigzag chain structure along the a-axis, built by purple polyhedra NiO_6, where gray, yellow-green and red balls represent Na, Te, and O atoms, respectively.

In this work, we overcame such drawbacks as poor crystal quality, small crystal size and internal impurities by adjusting the temperature schedule of the growth process and the ratio of raw materials, and successfully prepared pure bulk single crystals of Na_4MTeO_6 (M = Co, Ni) via the flux method, such that their quality fully meets the requirements for magnetic anisotropy measurements. To investigate the magnetic anisotropy and field-induced magnetic transition phenomena, we have tested the physical properties along different directions and calculated the distortion degrees of CoO_6 octahedra and NiO_6 octahedra. The results show that Na_4MTeO_6 (M = Co, Ni) are Ising-like antiferromagnets with strong magnetic anisotropy. Their Néel temperatures are 3.2 K and 6.5 K respectively, and both have the b-axis as the easy magnetic axis. Obvious spin-flips occur under a low magnetic field of 0–1 T for both compounds, and the distortion degree of CoO_6 octahedra is stronger than that of NiO_6 octahedra.

2. Experiment

Single crystals of Na_4MTeO_6 (M = Co, Ni) were successfully grown using a conventional flux method. The starting materials, Na_2CO_3 (99.5%, 8.4337 g), $Na_2MoO_4{\cdot}2H_2O$ (99.5%, 10.1715 g), transition-metal oxalate [$CoC_2O_4{\cdot}2H_2O$ (analytical grade, 10.0909 g) or $NiC_2O_4{\cdot}\ 2H_2O$ (99%, 6.5591 g)], and TeO_2 (4N, 6.0006 g for Co and 9.0009 g for Ni), were thoroughly mixed in stoichiometric ratios and placed into an alumina crucible.

For the growth of Na_4CoTeO_6, the mixture was heated to 1383 K and held for 10 h, followed by slow cooling to 1273 K at a rate of 0.5 K/h and then to room temperature at 100 K/h. For Na_4NiTeO_6, the mixture was heated to 1473 K for 6 h, cooled to 1373 K at 1 K/h, and finally cooled to room temperature at 100 K/h. After cooling, single crystals were mechanically separated from the flux and ultrasonically cleaned to remove any residual flux. The obtained Na_4CoTeO_6 crystals were well-shaped and reached a maximum size of approximately $3 \times 4 \times 3$ mm^3 (see Fig. 2(a)), while the Na_4NiTeO_6 crystals exhibited typical dimensions of about $0.8 \times 0.7 \times 0.5$ mm^3 (see Fig. 2(b)).

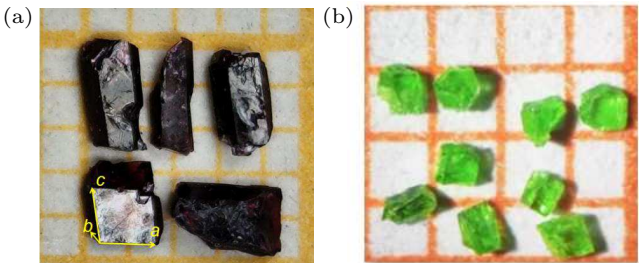


Fig. 2. Crystal samples of Na_4MTeO_6 (M = Co, Ni): (a) Na_4CoTeO_6 and (b) Na_4NiTeO_6.

The crystal structures of Na_4MTeO_6 (M = Co, Ni) were confirmed by single-crystal x-ray diffraction (XRD) (see Tables S1–S3). Magnetic susceptibility measurements were performed using a commercial magnetic property measurement system (MPMS) under an applied field of $H = 0.1$ T along the crystallographic a-, b-, and c-axes. Isothermal magnetization curves were collected using a Quantum Design physical property measurement system (PPMS) at $T = 2$ K with magnetic fields up to 8 T applied along the three principal axes.

3. Results and discussion

To investigate the fundamental magnetic properties of this family of compounds, we performed vibrating sample magnetometer (VSM) measurements on Na_4CoTeO_6. As shown in Fig. 3, under applied magnetic fields of 0.03 T and 0.1 T, the anisotropic magnetic susceptibility data of the single crystals exhibit consistent behavior at different magnetic field strengths, increasing uniformly with decreasing temperature, reaching a pronounced peak at approximately 3.2 K, followed by a sharp drop. This behavior indicates the onset of long-range antiferromagnetic ordering below 3.2 K, consistent with previous reports. The single-crystal data reveal pronounced magnetic anisotropy, with the susceptibility along the b-axis being the largest and that along the c-axis being the smallest, indicative of strong anisotropy. The high-temperature region of the susceptibility follows the Curie–Weiss law. Based on the data analysis under an external magnetic field of 0.03 T, the following parameters are derived: $\theta_{CW,a} = -4.50(6)$ K, $\mu_{eff,a} = 4.32(6)\ \mu_B$; $\theta_{CW,b} = 7.49(7)$ K, $\mu_{eff,b} = 5.49(3)\ \mu_B$;

$\theta_{CW,c} = -77.69(5)$ K, $\mu_{eff,c} = 3.88(4)$ μ_B. All three crystallographic directions display antiferromagnetic characteristics; however, the positive Curie–Weiss temperature along the *b*-axis suggests the presence of weak ferromagnetic interactions, which dominate along this direction, while antiferromagnetic interactions prevail along the *a*- and *c*-axes. Such anisotropic competition between ferromagnetic and antiferromagnetic interactions has also been observed in compounds like $LiVGe_2O_6$.[24] Moreover, the effective magnetic moments along all three axes exceed the theoretical value for Co^{2+} (3.87 μ_B, $S = 3/2$, $g = 2$), implying a significant orbital contribution to the total magnetic moment.

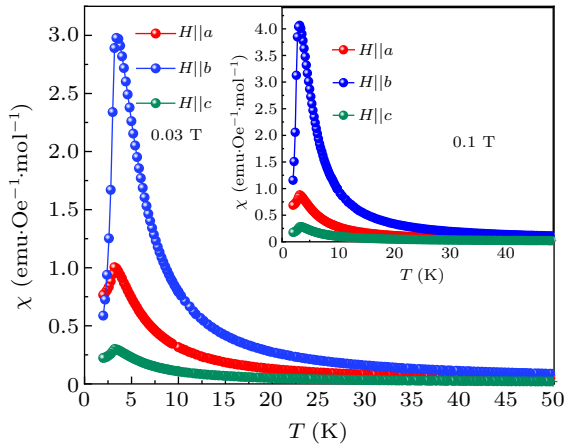


Fig. 3. Magnetic susceptibilities of Na_4CoTeO_6 measured along different axes under magnetic fields of 0.03 T and 0.1 T.

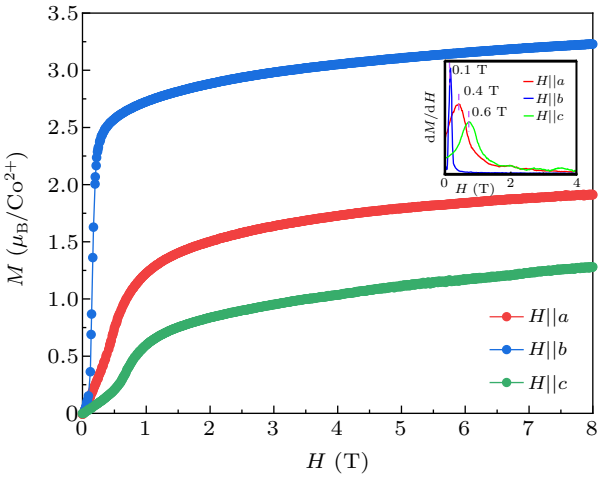


Fig. 4. Magnetization curves of Na_4CoTeO_6 measured along different axes at 2 K.

Figure 4 shows the field-dependent magnetization (*M*–*H*) curves of Na_4CoTeO_6 single-crystal samples measured at 2 K. In the low-field region, the magnetization increases linearly with the field, consistent with the characteristics of an antiferromagnetic ground state. A sudden increase in magnetization appears along the *b*-axis at approximately 0.1 T, followed by a gradual saturation; a similar jump is observed along the *a*-axis at around 0.4 T, while the spin-flip transition along the hard magnetization *c*-axis occurs at about 0.6 T. These results indicate a typical spin-flip transition under an applied magnetic field.[25] The *M*–*H* measurements further confirm that Na_4CoTeO_6 possesses strong magnetic anisotropy with the easy axis along the *b* direction.

To estimate the degree of anisotropy of Na_4CoTeO_6, we employed a simple uniaxial two-sublattice mean-field model.[25] When the direction of the applied magnetic field is parallel to the easy magnetization axis of the antiferromagnetic system, the spin magnetic moments tend to rearrange their orientation perpendicular to the magnetic field, resulting in an energy change of $\Delta E = 0.5H^2(\chi_\perp - \chi_\parallel)$. In cases where the magnetic anisotropy energy is low, the energy provided by the applied magnetic field can compensate for the anisotropy energy loss caused by the rearrangement of magnetic moments in the system. When the external field strength reaches the critical value H_{SF}, the spin orientation will undergo a spin-flip phase transition. Therefore, the anisotropy energy K is used to estimate the magnitude of the magnetic anisotropy energy, and its quantitative estimation can be performed using the empirical formula $K(T) = 0.5H_{SF}^2(\chi_\perp - \chi_\parallel)$. The magnetic susceptibilities parallel and perpendicular to the easy magnetization axis are taken as the values parallel to the *b*-axis and *c*-axis at 2 K, respectively, with $\chi_b = 2.98(2)$ emu/(mol·Oe) and $\chi_c = 3.01(3) \times 10^{-1}$ emu/(mol·Oe), given $H_{SF} = 0.11(1)$ T, the calculated value of $K(2\text{ K}) = 1.63(5) \times 10^5$ erg/cm^3,[26] which is lower than the 4×10^6 ergs/cm^3 reported in the literature for hcp Co.[27]

Figure 5 presents the temperature-dependent magnetic susceptibility (χ–T) of Na_4NiTeO_6 single crystals measured under applied fields of 0.03 T and 0.1 T. In contrast to Na_4CoTeO_6, the magnetic data of Na_4NiTeO_6 exhibit distinctly different behaviors under different external magnetic field strengths. At 0.03 T, the anisotropic magnetic susceptibility of the single crystal shows a consistent trend: it increases with decreasing temperature, reaches a peak at 5.9 K, and then decreases sharply. At 0.1 T, the *a*-axis and *b*-axis magnetic susceptibilities of the single crystal increase with decreasing temperature but continue to rise without showing a peak at 5.9 K. In contrast, the *c*-axis magnetic susceptibility of the single crystal behaves the same as that at 0.03 T, reaching a peak at 6.5 K. This indicates that an increase in the magnetic field strength induces spin flipping in Na_4NiTeO_6. At high temperatures, all curves follow the Curie–Weiss law. The parameters derived from the fitting process under an external magnetic field of 0.03 T are $\theta_{CW,a} = 13.01(1)$ K and $\mu_{eff,a} = 3.35(1)$ μ_B; $\theta_{CW,b} = 22.36(2)$ K and $\mu_{eff,b} = 3.42(5)$ μ_B; $\theta_{CW,c} = 15.22(4)$ K and $\mu_{eff,c} = 3.31(6)$ μ_B for the single crystal sample. The positive Curie–Weiss temperatures along the *a*- and *b*-axes suggest field-induced ferromagnetic tendencies under 0.03 T. The effective magnetic moments along all three axes exceed the spin-only value of 2.83 μ_B for Ni^{2+} ($S = 1$,

$g = 2$), implying a significant orbital contribution. The single-crystal measurements indicate that the b-axis is the easy magnetization direction.

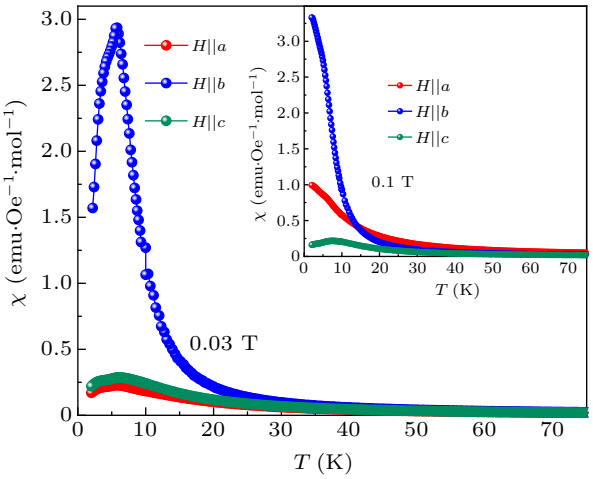


Fig. 5. Magnetic susceptibilities of Na_4NiTeO_6 measured along different axes under magnetic fields of 0.03 T and 0.1 T.

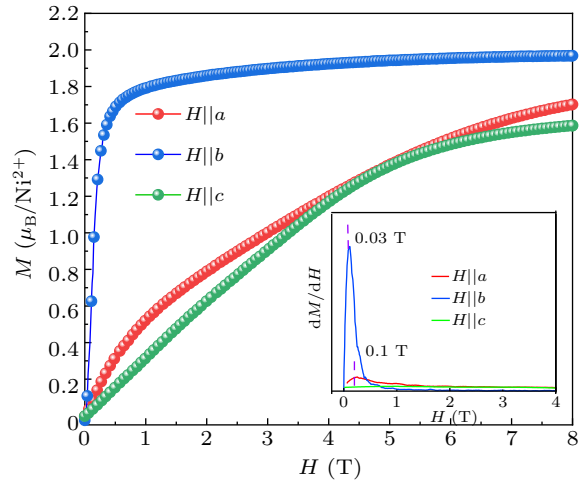


Fig. 6. Magnetization curves of Na_4NiTeO_6 measured along different axes at 2 K.

Figure 6 shows the M–H curves of Na_4NiTeO_6 at 2 K. In fields below 0.1 T, the magnetisation increases linearly along all axes, consistent with the antiferromagnetic ground state reported in previous susceptibility studies at 0.01 T.[23] A sharp jump in magnetisation is observed along the b-axis at around 0.03 T, followed by a gradual saturation above 0.4 T, indicating a spin-flip transition induced by the external field. Similar behaviour is also found along the a-axis near 0.1 T. Because the susceptibility measurements were performed under 0.1 T, the spins along the a- and b-axis have already undergone spin reorientation and exhibit a ferromagnetic alignment. This result reasonably accounts for the ferromagnetic-like behaviour observed in the magnetic susceptibility–temperature χ–T curves under an external magnetic field of 0.1 T. According to Ref. [23], the intrachain ferromagnetic coupling between Ni^{2+} ions is stronger than the interchain antiferromagnetic interaction. Therefore, even though the c-axis component remains antiferromagnetically coupled, the ferromagnetic contribution dominates, accounting for the positive θ_{CW} and antiferromagnetic-like response along the c-axis.

Na_4NiTeO_6 also exhibits strong magnetic anisotropy and undergoes a spin-flip transition under an external magnetic field. The higher spin-flip field along the hard magnetization c-axis further confirms that this compound, like Na_4CoTeO_6, is an Ising-like antiferromagnet. Notably, the appearance of Ising-like antiferromagnetic behavior in Ni-based oxides is relatively rare. Using the same model, with $\chi_b = 2.93(5)$ emu/(mol·Oe), $\chi_c = 2.29(3) \times 10^{-1}$ emu/(mol·Oe), and $H_{SF} = 3.5(2) \times 10^{-2}$ T, the anisotropy energy density is calculated to be $K(2\,\mathrm{K}) = 1.63(4) \times 10^4$ erg/cm^3, smaller than that of metallic Ni (8×10^5 erg/cm^3).[28]

In an ideal octahedral coordination environment, the orbital angular momentum of high-spin Co^{2+} and Ni^{2+} ions is expected to be quenched ($L = 0$), leading to negligible single-ion anisotropy and spin–orbit coupling. However, both Na_4MTeO_6 (M = Co, Ni) exhibit pronounced spin–orbit coupling, suggesting that structural distortions may play an essential role. To investigate this effect, we analysed the local distortion of the MO_6 (M = Co, Ni) octahedra and calculated their bond-length and bond-angle distortion parameters, ΔD and σ^2, according to the following equations:[29,30]

$$\Delta D = \sum \frac{D_i - D_{\mathrm{ave}}}{D_{\mathrm{ave}}} \times \frac{1}{n}, \tag{1}$$

$$\sigma^2 = \frac{1}{11} \sum_{i=1}^{12} (\alpha_i - 90)^2, \tag{2}$$

where D_i denotes the individual M–O bond length, D_{ave} is the average bond length, n is the total number of bonds, and α_i represents the O–M–O bond angle.

As summarised in Table 1, both the bond-length and bond-angle distortions for Co^{2+} are larger than those for Ni^{2+}, consistent with the estimated magnetic anisotropy energies. This result indicates that the enhanced structural distortion of the CoO_6 octahedra strengthens the spin–orbit coupling and contributes to the pronounced Ising-like system anisotropy in Na_4CoTeO_6.

Table 1. Degree of distortion ΔD ($\times 10^{-3}$), σ^2 and bond lengths for MO_6 (M = Ni, Co) octahedra.

Sites	D_{min}, D_{max} (Å)	ΔD	σ^2
Co	2.084, 2.155	14.81	87.63
Ni	2.099,2.1193	2.25	76.21

4. Conclusion and perspectives

In this study, large-sized high-quality single crystals of Na_4MTeO_6 (M = Co, Ni) were successfully grown, and their magnetic anisotropy and field-induced magnetic transitions were systematically investigated. Both Na_4CoTeO_6 and

Na_4NiTeO_6 are identified as Ising-like antiferromagnets exhibiting pronounced magnetic anisotropy. For Na_4CoTeO_6, the *b*-axis serves as the easy axis, and field-induced spin-flip transitions were observed along all three crystallographic directions, yielding a magnetic anisotropy constant of $K(2\ \mathrm{K}) = 1.63(5) \times 10^5$ erg/cm^3. Similarly, Na_4NiTeO_6 also shows the *b*-axis as the easy magnetisation direction, with spin-flip transitions occurring along both the *a*- and *b*-axes, and a calculated anisotropy constant of $K(2\ \mathrm{K}) = 1.63(4) \times 10^4$ erg/cm^3. Structural analysis further reveals that the CoO_6 octahedra exhibit greater bond-length and bond-angle distortions compared to NiO_6 octahedra, consistent with the observed stronger magnetic anisotropy in the Co compound.

Acknowledgment

This work was financially supported by the Self-deployed Key Project of State Key Laboratory of Functional Crystals and Devices (Grant No. GNJT-2025-ZD01).

References

[1] Bagnuls C and Bervillier C 1984 *J. Physique Lettres* **45** L95
[2] Newman C M and Stein D L 1990 *Phys. Rev. Lett.* **65** 460
[3] Lee J U, Lee S, Ryoo J H, Kang S, Kim T Y, Kim P, Park C H, Park J G and Cheong H 2016 *Nano Lett.* **16** 7433
[4] Fernandes R M, Chubukov A V and Schmalian J 2014 *Nat. Phys.* **10** 97
[5] Zhuang H L and Hennig R G 2016 *Phys. Rev. B* **93** 054407
[6] Krempasky J, Smejkal L, D'Souza S W, Hajlaoui M, Springholz G, Uhlírová K, Alarab F, Constantinou P C, Strocov V, Usanov D, Pudelko W R, González-Hernández R, Hellenes A B, Jansa Z, Reichlová H, Sobán Z, Betancourt R D G, Wadley P, Sinova J, Kriegner D, Minár J, Dil J H and Jungwirth T 2024 *Nature* **626** 517
[7] Baniodeh A, Lan Y H, Novitchi G, Mereacre V, Sukhanov A, Ferbinteanu M, Voronkova V, Anson C E and Powell A K 2013 *Dalton Trans.* **42** 8926
[8] Blatter G, Feigelman M V, Geshkenbein V B, Larkin A I and Vinokur V M 1994 *Rev. Mod. Phys.* **66** 1125
[9] Grenier B, Petit S, Simonet V, Canévet E, Regnault L P, Raymond S, Canals B, Berthier C and Lejay P 2015 *Phys. Rev. Lett.* **114** 017201
[10] Wang Z, Lorenz T, Gorbunov D I, Cong P T, Kohama Y, Niesen S, Breunig O, Engelmayer J, Herman A, Wu J D, Kindo K, Wosnitza J, Zherlitsyn S and Loidl A 2018 *Phys. Rev. Lett.* **120** 207201
[11] Wang Z, Wu J D, Yang W, Bera A K, Kamenskyi D, Islam A, Xu S L, Law J M, Lake B, Wu C J and Loidl A 2018 *Nature* **554** 219
[12] Shen L, Zaharko O, Birk J O, Jellyman E, He Z and Blackburn E 2019 *New J. Phys.* **21** 073014
[13] Cui Y, Zou H, Xi N, He Z Z, Yang Y X, Shu L, Zhang G H, Hu Z, Chen T, Yu R, Wu J D and Yu W Q 2019 *Phys. Rev. Lett.* **123** 067203
[14] Kimber S A J, Mutka H, Chatterji T, Hofmann T, Henry P F, Bordallo H N, Argyriou D N and Attfield J P 2011 *Phys. Rev. B* **84** 104423
[15] Liang T, Koohpayeh S M, Krizan J W, McQueen T M, Cava R J and Ong N P 2015 *Nat. Commun.* **6** 7043
[16] Lee S B, Kaul R K and Balents L 2010 *Nat. Phys.* **6** 702
[17] Coldea R, Tennant D A, Wheeler E M, Wawrzynska E, Prabhakaran D, Telling M, Habicht K, Smeibidl P and Kiefer K 2010 *Science* **327** 177
[18] Wu J D, Kormos M and Si Q M 2014 *Phys. Rev. Lett.* **113** 247202
[19] Greedan J, Munsie T, Thompson C, Dabkowska H, Luke G, Flacau R, Aczel A, Cao H B and Williams T 2017 *Acta Crystallogr. Sect. A* **73** A89
[20] Xiao G L, Li D, Niu H Y, Sun Z Y, Wang M, Song Y J, Xiao L X and Xia Z C 2023 *J. Phys. Chem. C* **6562** 6568
[21] He Z Z, Guo W B, Cui M Y and Tang Y Y 2017 *Dalton Trans.* **46** 5076
[22] He Z Z, Cui M Y and Qiu C Q 2018 *J. Alloy. Compd.* **748** 794
[23] Su C, Zeng X T, Li Y, Ma N, Lin Z W, Zhang C D, Wang C W, Chen Z Y, Lu X Y, Li W, Sheng X L and Jin W T 2022 *Sci. China-Phys. Mech. Astron.* **65** 227011
[24] Lumsden M D, Granroth G E, Mandrus D, Nagler S E, Thompson J R, Castellan J P and Gaulin B D 2000 *Phys. Rev. B* **62** R9244
[25] Lebeugle D, Colson D, Forget A, Viret M, Bataille A M and Gukasov A 2008 *Phys. Rev. Lett.* **100** 227201
[26] He Z, Taniyama T and Itoh M 2006 *Appl. Phys. Lett.* **88** 132506
[27] McGuire T R and Potter E C 1975 *J. Appl. Phys.* **46** 3920
[28] Bozorth R M 1951 *Ferromagnetism (New York: Van Nostrand)* p. 569
[29] Robinson K, Gibbs G V and Ribbe P H 1971 *Science* **172** 567
[30] Lang T C, Cai M S, Fang S Q, Han T, He S S, Wang Q Y, Ge G H, Wang J, Guo C Z, Peng L L, Cao S X, Liu B T, Korepanov V, Yakovlev A N and Qiu J B 2022 *Adv. Opt. Mater.* **10** 2101948